

# A Di-Higgs Search in the $\gamma\gamma b\bar{b}$ Decay Channel Using the ATLAS Detector

**Robert G. Reed, Stefan Von Bruddenbrock, Deepak Kar, Bruce Mellado**

School of Physics, University of the Witwatersrand, Johannesburg 2050, South Africa

E-mail: robert.reed@cern.ch

**Abstract.** The Higgs boson was discovered on July 4th 2012. The Higgs boson now offers a portal into physics beyond the Standard Model (BSM). The search for a di-Higgs production in the  $\gamma\gamma b\bar{b}$  decay channel is sensitive to extensions in the Standard Model and provides a way of probing new physics. In the  $\gamma\gamma b\bar{b}$  search using 2012 data an excess was seen around the 300 GeV mass of the four object ( $m_{\gamma\gamma b\bar{b}}$ ), although differing in the significance, for both ATLAS and CMS. The  $\gamma\gamma b\bar{b}$  channel is an early analysis which means the strategy and all associated frameworks must be ready as soon as possible. The first look at data will be to verify the excess seen in 2012 followed by a further investigation for BSM physics. This proceedings describes the implementation and overall status of the analysis framework developed for the  $\gamma\gamma b\bar{b}$  decay channel.

## 1. Introduction

The ATLAS and CMS Collaborations announced the discovery of a Higgs-like boson, on July 4<sup>th</sup> 2012, with a mass of 125 GeV [1,2]. After further studies using the full datasets available during Run I [3,4] this boson was observed to be consistent with the Standard Model (SM) Higgs Boson with a significance of  $10\sigma$  as seen in Fig. 1 [5]. The Standard Model predicts the Higgs boson as a consequence to spontaneous symmetry breaking which gives mass to elementary particles. The discovery and the measurement of its mass provides new means to probe physics that is beyond the Standard Model.

## 2. The ATLAS detector

The ATLAS detector is one of two main general purpose detectors at the LHC. The ATLAS detector is different in many respects to the CMS detector most noticeable is the air-core superconducting magnets that produce the toroidal field for the muon spectrometer. The detector is cylindrical in shape and has a forward-backward symmetry. The detector consists of concentric sub detectors. Starting from the inside we have the inner tracker and silicon micro-strip detector located inside the transition radiation tracker which provide tracking in the pseudorapidity<sup>1</sup> range  $|\eta| < 2.5$ , electromagnetic calorimeter and lead liquid-argon sampling device is divided into one barrel ( $|\eta| < 1.475$ ) and two end cap regions ( $1.375 < |\eta| < 3.2$ ), the

<sup>1</sup> In experimental particle physics, pseudorapidity,  $\eta$ , is a commonly used spatial coordinate describing the angle of a particle relative to the beam axis. It is define by  $\eta \equiv -\ln \left[ \tan \left( \frac{\theta}{2} \right) \right]$  where  $\theta$  is the angle between the particles three-momentum and the positive direction of the beam axis.

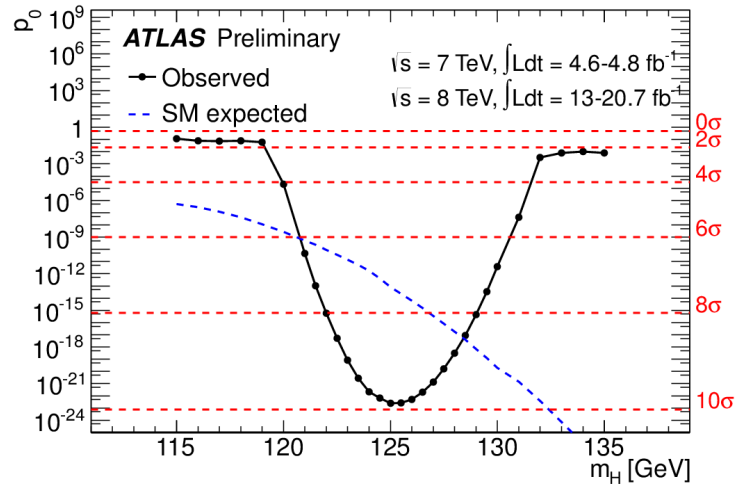


Figure 1: Combined search showing the local probability in the search for the standard Higgs boson [5]. The dashed line represents the Standard Model expected local probability.

hadron calorimeter is also divided into a barrel ( $|\eta| < 0.8$ ) and extended barrel ( $0.8 < |\eta| < 1.7$ ) both of which consist of steel and plastic scintillators. Each sub detector is designed to identify different particles, their energies and trajectories. All signals from the sub-detectors are used to reconstruct the event and all particles that are produced in the collision. The reconstructed data is then processed by various analysis groups to look for interesting physics such as that found beyond the SM. The Higgs boson opens a portal to study physics beyond the SM by making use of particular decay channels which are sensitive to extensions of the SM theory. Such a channel is the di-Higgs to  $\gamma\gamma b\bar{b}$  which is a sub analysis of the Higgs to  $\gamma\gamma$  group.

### 3. The $\gamma\gamma b\bar{b}$ run I results

The  $\gamma\gamma b\bar{b}$  final state search is an excellent channel for Higgs boson pair production searches due to the large branching ratio of the  $h \rightarrow b\bar{b}$  process [6]. Combining the large branching ratio with the clean di-photon trigger, di-photon mass resolution and low background we get a very clean analysis. Figure 2 shows the 95% Confidence Limit (CL) on the cross section times the branching ratios of a narrow resonance decaying into two Higgs bosons [7]. It is immediately clear there is an excess around the  $m_X \approx 300$  GeV area, where  $m_X$  is the mass of the heavy mediator. The CMS detector also observed an excess in a similar region but with a smaller significance [8]. The excess in itself warrants further investigation, due to the presence in both CMS and ATLAS, which will be the driving factor in the early data collection of Run 2 for this decay channel. The framework described in following sections will attempt to verify if this excess still exists in the 2015 data taking period (Run II) using the new data formats.

### 4. Run II $\gamma\gamma b\bar{b}$ analysis framework

The  $\gamma\gamma b\bar{b}$  framework inherits its core functionality from its parent analysis group. This means the calibration and event selection is largely pre-defined by the  $\gamma\gamma$  group. I will focus on how the sub analysis differs from the di-photon analysis which is described in Ref. [1,4]. All analysis groups are using the new xAOD data format that is the standard in ATLAS. The analysis code is written in c++11 using an object orientated approach. This allows a central repository of tools which can be used by many groups allowing more eyes to debug the same code. The  $\gamma\gamma$  group has written a core analysis code which sub groups can inherit from allowing centralised

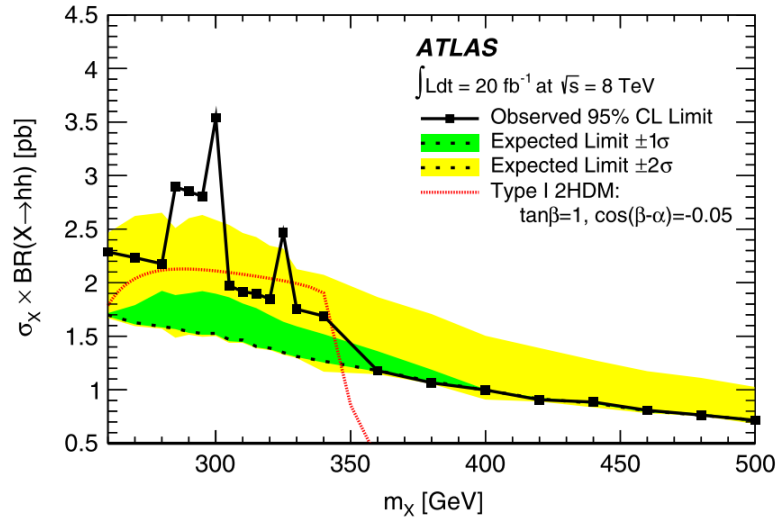


Figure 2: A 95 % CL upper limit on the cross section times branching ratios of a narrow resonance decaying to pairs of Higgs bosons as a function of  $m_X$  [7].

calibration and selections across all sub groups. The difference in the object selection between the  $\gamma\gamma b\bar{b}$  and  $\gamma\gamma$  groups can be described on an object by object basis.

#### 4.1. Photons

There is no difference in photon selection from the  $\gamma\gamma$  group as the  $\gamma\gamma b\bar{b}$  analysis is an extension including two jets (a narrow cone of hadronic material and possibly other particles produced by the hadronisation of a quark or gluon during a collision) formed from  $b$ -quarks these are flavored jets called BJets.

#### 4.2. Electrons

Since electrons are not of interest we follow the same recommendations as the  $\gamma\gamma$  group.

#### 4.3. Jets

The primary focus in the  $\gamma\gamma b\bar{b}$  channel is the identification of jets formed by  $b$  quarks. Jets are required to be in the central region  $|\eta| < 2.5$  for better  $b$ -tagging efficiency. A tighter cut on the Jet Vertex Fraction (JVF) of 0.5 is applied which is different to the  $\gamma\gamma$  cut of 0.25. The JVF discriminant measures the probability that a jet originated from a particular vertex. This is important for  $b$ -tagging reasons due to the displaced secondary vertex caused by  $b$ -mesons in the  $b$ -jet identification. In the latest derivation of data production the JVF will be replaced by a new Jet Vertex Tagger (JVT) which is expected to perform better. Finally, the jet is required to have a transverse momentum greater than 25 GeV.

#### 4.4. Muons

Muons are selected in a similar way to the  $\gamma\gamma$  analysis. Muons are rejected if they overlap any jet unless that jet is in fact a  $b$ -tagged jet. In the case a muon overlaps a  $b$ -tagged jet we add the four momentum of the muon to the jet.

#### 4.5. $b$ -jets

Jets are tagged by flavour using multivariate analysis techniques. A new tagging tool is used to perform this classification but an additional variable is saved using the Run I tool for comparison.

A 70% working point is used for  $b$ -tagged jet classification. Events are rejected if the leading (sub)  $b$ -jets have transverse momentum less than 55 (35) GeV. The invariant mass of the dijet system must be within the mass window 95 GeV - 135 GeV. The value of the  $b$ -tagging working point is currently the same as Run I for comparisons but this has yet to be optimised.

### 5. Configuring the framework

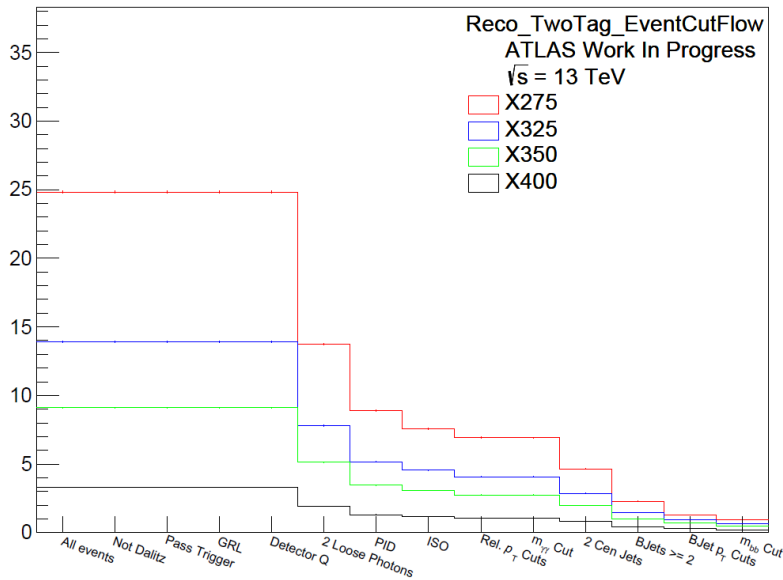


Figure 3: The cutflow produced by the  $\gamma\gamma b\bar{b}$  framework.

In order to steer the analysis we use configuration files which are used to setup the analysis code to perform the desired function. Figure 4 shows the different options available to the user. The benefit of using such configuration files is that the user can change cut values or tagging working points without having to edit the source code and recompile. This feature makes the framework user friendly and flexible to different needs. In the latest release there are over 58 different parameters that can be tuned in the configuration file and this is likely to grow as we keep adding features.

Flag	Default	Description
<b># Photon Selection</b>		
HH2yybb.PhotonSelection.ApplyFakePhotonWeights	NO	Add fake photon event weights (Ongoing)
<b># BTagging Selection</b>		
JetHandler.EnableBTagging:	YES	Turn Btagging on/off
JetHandler.Selection.RemoveBJets:	NO	Remove all bjets
JetHandler.Selection.SelectBJets:	NO	Keep only bjets
JetHandler.Selection.BTagOperatingPointNames:	MV1_60 ...	MV1 working point names
JetHandler.Selection.BTagOperatingPointCuts:	0.991565 ...	Actual MV1 cut value
HH2yybb.Selection.UseWorkingPoint:	MV1_70	Selected working point to use
JetHandler.Selection.BTagAbsRapidity:	2.5	Cut on btagging range

Figure 4: An example of some options available to the user in the configuration file. Over 60 different features are available.

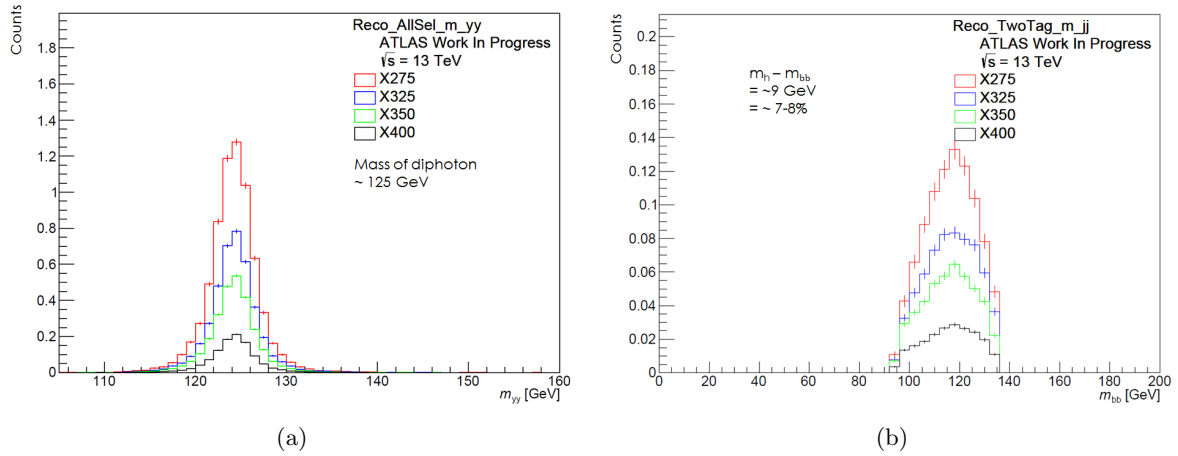


Figure 5: a) Invariant mass of di-photons and b) di- $b$ -jets for four different signal samples.

## 6. Preliminary results

### 6.1. Cutflow

Figure 3 shows the cutflow produced by the framework for four different Monte-Carlo signal simulations. Each simulation has a different mass for the heavy scalar ( $X$ ). Events are rejected at each cut level. The final cut is the mass window of the  $b\bar{b}$  object. Any event passing this cut will be a candidate for the four object  $\gamma\gamma b\bar{b}$ .

### 6.2. Invariant mass of $\gamma\gamma$ and $b\bar{b}$

Figure 5 a) shows the invariant mass of the selected di-photons and di- $b$ -jets. The  $m_{\gamma\gamma} \approx 125 \text{ GeV}$  which indicates the framework is selecting the correct photons from the decay of one of the Higgs. In the case of the di- $b$ -jet mass, Fig. 5 b), we see a slight underestimate ranging between 7 – 8% with a value of  $m_{b\bar{b}} \approx 120 \text{ GeV}$ . The slight under estimate can be studied by looking at the ratio between the reconstructed energy,  $E_{Reco}$ , to the energy of the  $b$ -quark,  $E_{bquark}$ . This is called the jet response.

### 6.3. $b$ -jet response

The  $b$ -jet response, defined by  $Response = (E_{RecoBJet} - E_{bquark})/E_{bquark}$ , is a relative indication of how far above or below the reconstructed  $b$ -jet energy is to the truth energy of the  $b$ -quark. This is useful for calibrations specific to  $b$ -jets for the  $\gamma\gamma b\bar{b}$  analysis. Its only applicable when looking at simulations since the truth information is not available in actual data. Figure 6 shows the response calculated for all  $b$ -jets matched to their respective  $b$ -quark. The mean value of  $-0.078$  reflects the negative 7 – 8% we saw in Fig. 5 b). An asymmetric Gaussian is fitted which predicts the mean values of the peak as well as the width above and below the mean. It turns out that the response is dependant on the transverse momentum  $p_T$  and the pseudorapidity  $\eta$ . Further studies need to be done to investigate this dependence.

## 7. Discussion and Conclusions

This framework will provide the platform necessary to perform statistical procedures to verify the existence of the excess seen in Run I. Physics data is expected to be produced at 25 ns by August 2015 which means the framework and all associated statistical machinery must be ready and in place. The analysis framework is in a mature stage of development and the results shown provide verification that it is performing as expected. Work that will follow this advancement

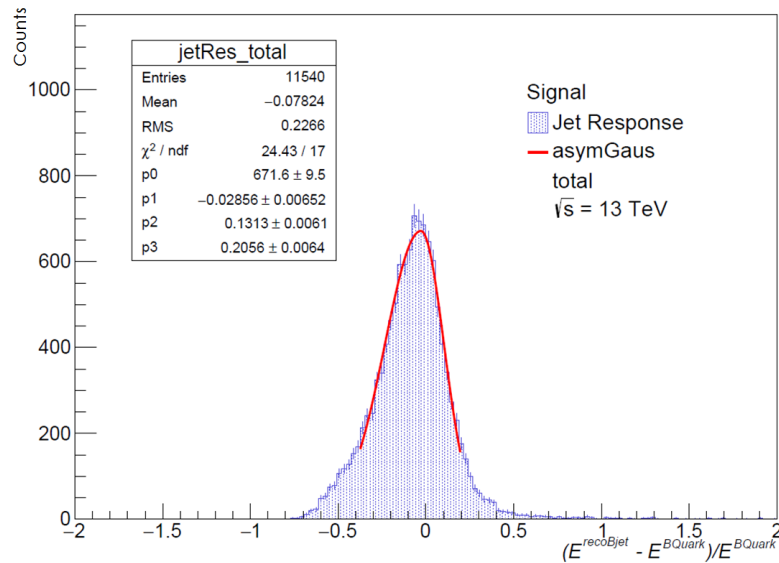


Figure 6: Total  $b$ -jet response with asymmetric Gaussian fit

will be the understanding and development of the statistical machinery that will be used for limit setting and local probability calculations. Further studied will be done on the  $b$ -jet response and the impact it will have on the  $m_{\gamma\gamma b\bar{b}}$  distribution. The framework as it stands is largely ready for the Run 2 data taking period. This framework will be used by members of the  $\gamma\gamma$  group and any sub group which may benefit from  $b$ -tagging functionality.

## 8. Acknowledgements

The National Research Foundation for the bursary they provided. The Department of Science and Technology and the SA-CERN program who provided financial assistance for research visits to CERN. We would also like to thank the School of Physics, the Faculty of Science and the Research Office at the University of the Witwatersrand.

## References

- [1] The ATLAS Collaboration 2012 *Physics Letters B* **716** 1–29
- [2] The CMS Collaboration 2012 *Physics Letters, Section B: Nuclear, Elementary Particle and High-Energy Physics* **716** 30–61
- [3] The CMS Collaboration 2014 *The European Physical Journal C* **74** 3076
- [4] The ATLAS Collaboration 2012 *Phys. Rev. Lett.* **108** **111803** 1–19
- [5] The ATLAS Collaboration 2013 *ATLAS-CONF-2013-034*
- [6] Heinemeyer S, *et al.* 2013 *CERN-2013-004, FERMILAB-CONF-13-667-T*
- [7] The ATLAS Collaboration 2015 *Physical Review Letters* **114** 081802
- [8] CMS Collaboration 2014 *CMS PAS HIG-13-032*